Redox Biology 6 (2015) 578–586

Contents lists available at ScienceDirect

Redox Biology

journal homepage: www.elsevier.com/locate/redox

Research Paper

Ovarian endometriosis-associated stromal cells reveal persistently high affinity for iron

Masahiko Mori [a,b], Fumiya Ito [a], Lei Shi [a], Yue Wang [a], Chiharu Ishida [a,b], Yuka Hattori [c], Masato Niwa [d], Tasuku Hirayama [d], Hideko Nagasawa [d], Akira Iwase [b], Fumitaka Kikkawa [b], Shinya Toyokuni [a,*]

[a] Department of Pathology and Biological Responses, Nagoya University Graduate School of Medicine, 65 Tsurumai-cho, Showa-ku, Nagoya 466-8550, Japan
[b] Department of Obstetrics and Gynecology, Nagoya University Graduate School of Medicine, Nagoya, Japan
[c] Department of Obstetrics and Gynecology, Nagoya Ekisaikai Hospital, Nagoya, Japan
[d] Laboratory of Pharmaceutical and Medical Chemistry, Gifu Pharmaceutical University, Gifu, Japan

ARTICLE INFO

Article history:
Received 2 September 2015
Accepted 10 October 2015

Keywords:
Ovarian endometriosis
Stromal cells
Catalytic ferrous iron
Transferrin receptor
Ferroportin

ABSTRACT

Ovarian endometriosis is a recognized risk for infertility and epithelial ovarian cancer, presumably due to iron overload resulting from repeated hemorrhage. To find a clue for early detection and prevention of ovarian endometriosis-associated cancer, it is mandatory to evaluate catalytic (labile) ferrous iron (catalytic Fe(II)) and to study iron manipulation in ovarian endometriotic lesions. By the use of tissues from women of ovarian endometriosis as well as endometrial tissue from women with and without endometriosis, we for the first time performed histological analysis and cellular detection of catalytic Fe(II) with a specific fluorescent probe (HMRhoNox-M), and further evaluated iron transport proteins in the human specimens and in co-culture experiments using immortalized human eutopic/ectopic endometrial stromal cells (ESCs) in the presence or absence of epithelial cells (EpCs). The amounts of catalytic Fe(II) were higher in ectopic endometrial stromal cells (ecESCs) than in normal eutopic endometrial stromal cells (n-euESCs) both in the tissues and in the corresponding immortalized ESCs. ecESCs exhibited higher transferrin receptor 1 expression both *in vivo* and *in vitro* and lower ferroportin expression *in vivo* than n-euESCs, leading to sustained iron uptake. In co-culture experiments of ESCs with iron-loaded EpCs, ecESCs received catalytic ferrous iron from EpCs, but n-euESCs did not. These data suggest that ecESC play a protective role for cancer-target epithelial cells by collecting excess iron, and that these characteristics are retained in the immortalized ecESCs.

1. Introduction

Endometriosis is an estrogen-dependent chronic inflammatory disease in which epithelial and stromal cells similar to the normal endometrial structure exist outside the uterine cavity [1–3]. The morbidity of endometriosis reaches 6–10% in women of reproductive age, and the patients suffer from dysmenorrhea, dyspareunia, chronic pelvic pain and infertility [1–3]. Furthermore, it is recognized that ovarian endometriosis is a risk factor for ovarian cancer such as clear cell adenocarcinoma and endometrioid adenocarcinoma [4,5].

Ovarian endometriosis causes local iron deposition due to repeated monthly hemorrhage [6,7]. Iron is the most abundant heavy metal in the human body and is essential as an oxygen transporter and a cofactor for various enzymes [8]. However, iron excess increases catalytic iron and leads to different classes of diseases, including diabetes mellitus [9], liver cirrhosis [10] and cancer [6]. Catalytic ferrous iron (catalytic Fe(II)) reacts with hydrogen peroxide to produce the hydroxyl radical in a Fenton reaction [11,12]. Hydroxyl radicals not only react with lipids and proteins but also causes oxidative damage to DNA, resulting in base modifications and strand breaks [13–16]. Endometriotic cysts present extremely high concentrations of catalytic iron compared with normal serum and the contents of other ovarian tumors. Indeed, the epithelia covering endometriotic cysts contain a high level of oxidative DNA damage compared with other ovarian tumors [17,18], which may be a major pathology for carcinogenesis [19,20].

Abbreviations: ESCs, endometrial(-otic) stromal cells; ecESCs, ectopic ESCs (immortalized); e-euESCs, eutopic ESCs with endometriosis (immortalized); n-euESCs, eutopic ESCs without endometriosis (in controls, immortalized); EpCs, epithelial cells; Fe-NTA, ferric nitrilotriacetate; IRP, iron regulatory protein or iron-responsive element binding protein; TfR1, transferrin receptor 1

* Corresponding author. Fax: +81 52 744 2091.
E-mail address: toyokuni@med.nagoya-u.ac.jp (S. Toyokuni).

http://dx.doi.org/10.1016/j.redox.2015.10.001

Recently, a highly specific fluorescent probe for catalytic (labile) Fe(II), named RhoNox-1, was developed [21]. Recently, we reported on an increase in catalytic Fe(II) in the target cells of a rat model of iron-induced renal cancer [22] and in amniotic fluid of human maternal-fetal disorders [23], using RhoNox-1. Furthermore, a new class of high-contrast fluorescent probes for catalytic Fe(II), called HMRhoNox-M, in which the turn-on contrasts were significantly improved compared with those of RhoNox-1, was described [24].

Mesenchymal tissue, represented by bone, cartilage, muscle and adipose tissue, not only connects and supports organs but also forms scaffolds for epithelial cells, thus playing a role in physiological functions. The Müllerian duct is a mesodermal precursor of the female genital tract, from which the uterus originates. The Müllerian duct comprises mesoepithelia and the mesenchyme surrounding them. Thus, endometrial epithelia originate from mesoepithelia, whereas endometrial stroma originate from the surrounding mesenchyme [25,26]. Of note, erythrocytes and skeletal muscle, derived from mesoderm and mesenchyme, use a large amount of iron for oxygen transport and storage. Liver, derived from endoderm, is the largest iron storage organ. However, mesenchymal stem cells can reportedly differentiate into hepatocytes [27], thus indicating a link between mesoderm and iron storage.

The relationship between endometriosis and catalytic Fe(II) are presently unknown. Here, for the first time, we studied the localization of catalytic Fe(II) in endometriotic lesions and the associated endometrial(-otic) stromal cells with a selective turn-on fluorescent probe for catalytic Fe(II) to consider a possible role of ectopic endometrial stromal cells as a storage site for excess iron.

2. Materials and methods

2.1. Materials

HMRhoNox-M was prepared according to the reported procedure [24]. We purchased iron (III) chloride hexahydrate (Wako, Osaka, Japan), LysoTracker (Molecular Probes, Eugene, OR), MitoTracker (Molecular Probes), CellTracker Green CMFDA (Molecular Probes), Hoechst 33342 (Molecular Probes), Cellmatrix Type I-P collagen (Nitta Gelatin, Inc., Osaka, Japan), anti-human transferrin receptor antibody (Zymed, 13-6800; San Francisco, CA), anti-ferroportin 1 antibody (Novus Biologicals, NBP1-21502; Littleton, CO), anti-CD10 monoclonal antibody (Novocastra, NCL-L-CD10-270; Newcastle, UK), anti β-actin monoclonal antibody (Wako, 011-24554; Tokyo, Japan), Stealth siRNAs for human transferrin receptor 1 (TfR1) (HSS110674, HSS110676 and HSS186305) and a non-targeting siRNA (HSS12935-112) as a negative control (Invitrogen, Carlsbad, CA). We prepared ferric nitrilotriacetate (Fe (III)-NTA) solution by mixing 300 mM ferric nitrate and 600 mM nitrilotriacetate, followed by pH adjustment to 7.4 with sodium hydrogen bicarbonate as described [28]. The other chemicals were of analytical grade.

2.2. Prussian blue staining

Prussian blue staining to detect insoluble iron was performed with freshly prepared 2% potassium ferrocyanide and 2% hydrochloric acid. Following a 30 min incubation, the sections were rinsed in water and counterstained with nuclear fast red, dehydrated, and covered. The slide images were captured with a BZ-9000 microscope (Keyence, Osaka, Japan).

2.3. Histological analysis of catalytic ferrous iron

HMRhoNox-M was stored at −80 °C and dissolved in dimethylsulfoxide to produce a 10 mM solution, which was further diluted (1:1000) with 10 mM phosphate-buffered saline (pH 7.2) (PBS) before use to a final concentration of 10 μM. Frozen sections were cut at a thickness of 8 μm with a cryostat onto MAS-GP type A grass slides (Matsunami, Osaka, Japan), air dried for 5 min, fixed for 3 min in 10 mM PBS-buffered 20% formalin in methanol, and washed for 5 min in PBS. Thereafter, an ample amount of 10 μM HMRhoNox-M was applied on these specimens, followed by incubation for 30 min at 37 °C in a dark box and rinse in PBS. Then, the specimens were counterstained with Hoechst 33342 and captured with a BZ-9000 microscope.

2.4. Cell culture experiments

Endometrial(-otic) stromal cells were established using E6, E7 and hTERT (lentiviruses and retroviruses) as previously described [29–31]. Immortalized endometrial stromal cells were maintained in phenol red Dulbecco's modified Eagle's medium (DMEM) (Sigma, St. Louis, MO) containing 10% fetal bovine serum (Biological Industries, Beit Haemek, Israel), 100 IU/mL of penicillin, 100 mg/L of streptomycin and 25 mg/L of amphotericin B. A well-differentiated human endometrioid adenocarcinoma cell line named "Ishikawa" was a generous gift from Dr. Masato Nishida (Kasumigaura Hospital, Ibaraki, Japan) [32]. Ishikawa cells, as a model of endometrial epithelial cells (EpCs), were maintained in RPMI 1640 (Sigma) containing 10% fetal bovine serum, 100 IU/mL of penicillin and 100 mg/L of streptomycin. These cells were incubated at 37 °C in a humidified atmosphere of 5% CO_2, as previously described [31]. In the present study, immortalized normal eutopic endometrial stromal cells, immortalized eutopic endometrial stromal cells of endometriosis and immortalized ectopic endometrial stromal cells were abbreviated as n-euESCs, e-euESCs and ecESCs, respectively. Three cell lines from different patients, respectively, were established, and data were collected at least in triplicate.

2.5. Patients and human samples

The ethics committee (internal review board) of the Nagoya University Graduate School of Medicine approved the experiments (no. 4884). Written informed consent was obtained from each patient before sampling. Paraffin-embedded tissues of ovarian endometriosis from three patients, endometrium from three patients with endometriosis and endometrium from three patients without endometriosis who had been resected for therapeutic purposes at Nagoya University Hospital were used for immunohistochemical analyses. Tissues of ovarian endometriosis for frozen section were obtained from three patients with endometriosis. Tissues of adenomyosis for frozen section were obtained from one patient. Normal endometrial tissues for frozen section were obtained from three patients with Stage IA1 or IB1 cervical adenocarcinoma without endometriosis.

2.6. Immunohistochemistry

All samples were fixed in 10 mM PBS-buffered 10% formalin and embedded in paraffin, and sections were cut at a thickness of 4 μm. For antigen retrieval, the sections, following deparaffinization, were heated at 95 °C in Tris-EDTA buffer (10 mM Tris base, 1 mM EDTA solution, pH 9.0) with a microwave oven for 20 min. Immunohistochemical staining was performed by employing the avidin-biotin immunoperoxidase technique using the Histofine SAB-PO kit (Nichirei, Tokyo, Japan) according to the manufacturer's protocol. Endogenous peroxidase activity was blocked by

incubation with 0.3% H_2O_2 in methanol for 20 min, and nonspecific immunoglobulin binding was blocked by incubation for 10 min in 10% normal serum in PBS with the corresponding species of the secondary antibody. The sections were incubated at 4 °C overnight with anti-human transferrin receptor antibody (1:500), anti-ferroportin 1 antibody (1:1000) and anti-CD10 (1:50). The sections were then rinsed and incubated with biotinylated secondary antibody for 10 min. After washing with PBS, the sections were incubated with horseradish peroxidase-conjugated streptavidin for 5 min and finally treated with diaminobenzidine in 0.01% H_2O_2 for 5 min. The slides were counterstained with Meyer's hematoxylin. Whole slide images were captured with a BZ-9000 microscope.

2.7. Morphological analyses with LysoTracker/MitoTracker and HMRhoNox-M

n-euESCs, e-euESCs and ecESCs (ESCs) were incubated for 30 min at 37 °C with 250 nM LysoTracker or 50 nM MitoTracker in Hank's balanced salt solution (HBSS) (GIBCO, Carlsbad, CA), rinsed in HBSS and incubated for 30 min at 37 °C with 10 μM of HMRhoNox-M with HBSS, followed by rinse in HBSS and observation with a confocal laser microscope, TiEA1R (Nikon Instech Co., Tokyo, Japan). The fluorescence intensity of HMRhoNox-M and LysoTracker/MitoTracker in the cytoplasm was quantified with NIS-Elements imaging software (Nikon Instech Co.).

2.8. Protein extraction techniques and western blot analysis

Protein extraction techniques and western blot analysis were performed as described [33]. Briefly, ESCs were washed with PBS, lysed in RIPA buffer [10 mM Tris–HCl (pH 7.4), 150 mM NaCl, 1% Nonidet P-40, 5 mM EDTA, 1% sodium deoxycholate, 0.1% sodium dodecyl sulfate (SDS), 1.2% aprotinin, 5 μM leupeptin, 4 μM antipain, 1 mM phenylmethyl sulfonyl fluoride, and 0.1 mM Na_3VO_4], homogenized on ice, centrifuged at 20,630*g* at 4 °C for 20 min, and diluted in 2x sample buffer [125 mM Tris–HCl (pH 6.8), 4% SDS, 10% glycerol, 0.2% bromophenol blue and 4% 2-mercaptoethanol]. After boiling at 95 °C for 5 min, the samples were analyzed with 10% SDS-polyacrylamide gel electrophoresis (PAGE). The proteins separated by SDS-PAGE were transferred to polyvinylidene difluoride (PVDF) membrane, followed by incubation for 1 h with 5% skim milk in Tris-buffered saline containing 0.05% Tween 20. The membrane was then incubated overnight at 4 °C with primary antibody; anti-transferrin receptor antibody (1:2000) or anti-β-actin antibody (1:3000). The membrane was washed three times with Tween-PBS for 10 min, followed by incubation with anti-mouse IgG HRP-linked antibody (#7076 S, 1:2000; Cell Signaling Technology, Danvers, MA) as a secondary antibody for 1 h. After washing with Tween-PBS, the membrane was reacted with Amersham ECL Western blot detecting reagent (GE Healthcare, Buckinghamshire, UK) and the chemiluminescence was detected. β-actin was used as an internal control.

2.9. Iron loading and transfer experiment under co-culture of ESCs and epithelial cells

Either epithelial cells (EpCs; Ishikawa cells) or ESCs were incubated in the corresponding medium with 50 μM $FeCl_3$ or Fe(III)-NTA for 12 h, while the cells that were not exposed to iron were incubated in serum-free medium for 12 h. ESCs were labeled with 2 μM CellTracker Green CMFDA for the final 1 h according to the manufacturer's protocol. EpCs and ESCs were mixed and seeded at 3.5×10^5 cells, each, per 35 mm glass-base dish (IWAKI, Tokyo, Japan) coated with collagen (Cellmatrix Type I–P), according to the manufacture's protocol. After 6 h, the mixed cells were incubated with 10 μM of HMRhoNox-M in HBSS for 1 h and counterstained with Hoechst 33342 for 30 min. Then, the images were captured with a BZ-9000 microscope.

2.10. RNA interference

TfR1 expression was silenced with three siRNA preparations. Three siRNAs targeting human *TfR1* sequences and a non-targeting siRNA, as a negative control per the manufacturer's recommendation, were purchased as described. ecESCs were seeded at 2.5×10^6 cells per 60 mm collagen-coated dish, incubated in DMEM with 10% FBS for 12 h, and then incubated in DMEM without serum for 24 h. This was followed by transfection with each siRNA (30 nM) with Lipofectamine RNAiMAX according to the manufacturer's protocol. The media was changed to DMEM with 10% FBS after 24 h. Silencing of *TfR1* expression was confirmed at 48 h with western blot analysis. Data were collected using three different ecESCs.

2.11. Statistical analysis

Date is shown as the mean ± SEM. A one-way ANOVA test followed by a Tukey HSD test or an unpaired Student's *t*-test was applied using SPSS version 22.0 (SPSS Inc., Chicago, IL). $P < 0.05$ was considered statistically significant.

3. Results

3.1. Distribution of catalytic Fe(II) in human specimens

ecESCs of endometriotic cysts revealed the strongest HMRhoNox-M fluorescence, indicating an abundance of catalytic Fe(II) (Fig. 1a–h). The localization of hemosiderin was independent of that of catalytic Fe(II) iron (Fig. 1g–j). Normal endometrium showed a small amount of catalytic Fe(II) (Fig. 1k–n). ecESCs of adenomyosis within the uterine muscle layer showed a larger amount of catalytic Fe(II) compared with the euESCs (Fig. 1o–r).

3.2. Intracellular localization of catalytic Fe(II) in ESCs

Catalytic Fe(II) in the immortalized ESCs as seen by HMRhoNox-M was mostly located in lysosomes, and partially in mitochondria (Supplemental Fig. 1). There was no significant difference in the distribution of lysosomes, mitochondria and the associated catalytic Fe(II) among different ESCs.

3.3. Effects of iron loading on catalytic Fe(II) in ESCs

We then evaluated the alteration of catalytic Fe(II) in n-euESCs, e-euESCs and ecESCs after treatment with 0, 10, 25 and 50 μM $FeCl_3$ for 6 h (Fig. 2A). At any dose of $FeCl_3$, ecESCs and e-euESCs showed high catalytic Fe(II) compared with that of n-euESCs. Catalytic Fe(II) of endometriosis-associated stromal cells (ecESCs and e-euESCs) increased in a dose-dependent manner up to 50 μM $FeCl_3$. In contrast, catalytic Fe(II) of n-euESCs increased at 10 μM $FeCl_3$ but decreased at 25 and 50 μM $FeCl_3$. Simultaneously we performed a time-course study on catalytic Fe(II) in n-euESCs, e-euESCs and ecESCs after treatment with 50 μM $FeCl_3$ (Fig. 2B). At any time after $FeCl_3$ treatment, endometriosis-associated stromal cells presented higher catalytic Fe(II) than that of n-euESCs. Catalytic Fe(II) of ecESCs increased in a time-dependent manner. However, catalytic Fe(II) of n-euESCs and e-euESCs increased with

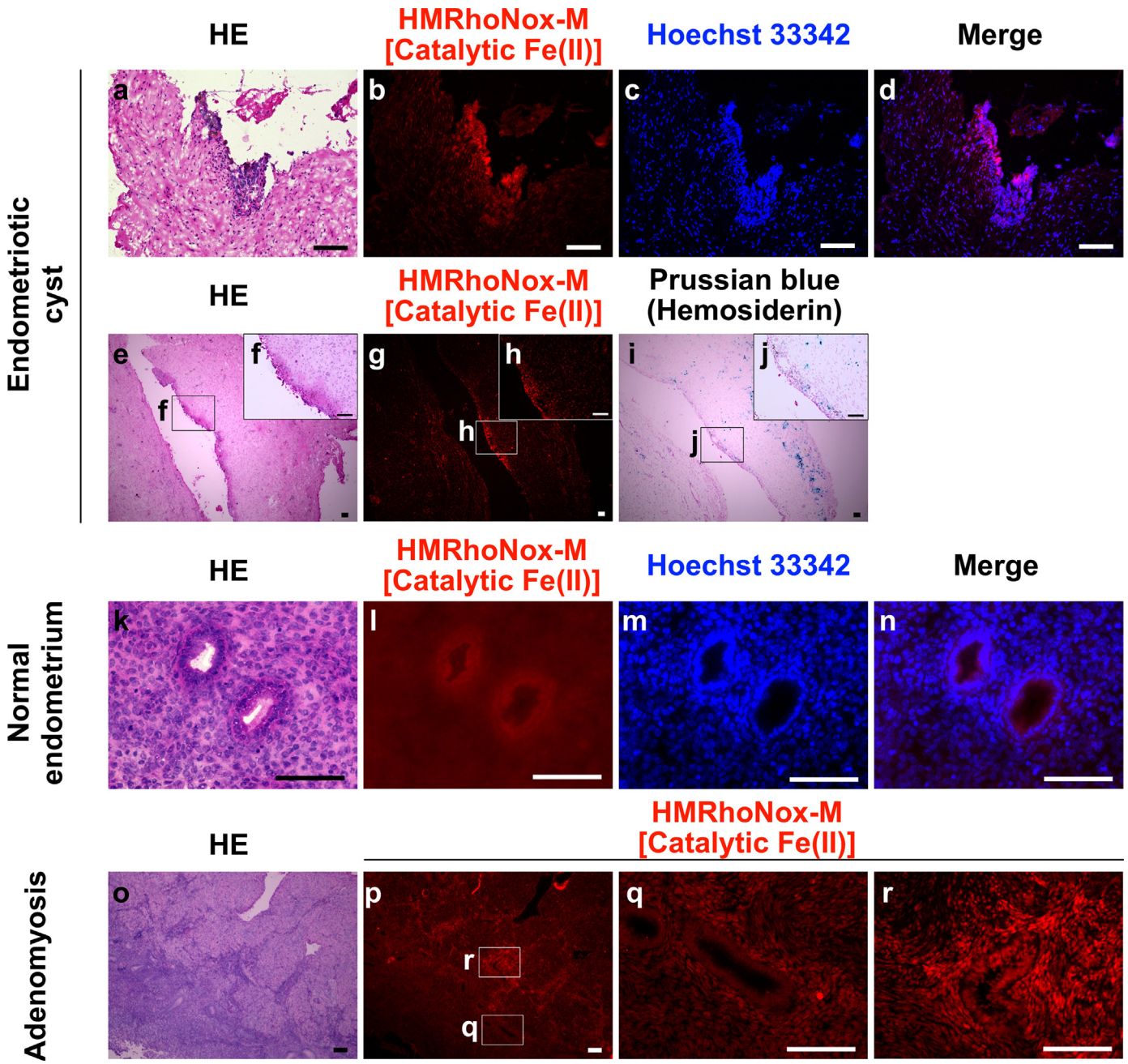

Fig. 1. Abundant catalytic ferrous iron (catalytic Fe(II)) is detected in endometriotic tissue in the ovary and in adenomyosis lesions within the uterine muscle layer. We performed histological detection for catalytic Fe(II) with HMRhoNox-M. The frozen sections of a–j, k–n and o–r are generated from endometriotic cysts, normal endometrium and endometrium of adenomyosis, respectively. Hematoxylin and eosin staining of ectopic or eutopic endometrial epithelium and stroma (a, e, f, k, o). HMRhoNox-M fluorescent staining of catalytic Fe(II) (b, g, h, l, p, q, r). Hoechst 33342 nuclear staining (c, m). Merged with catalytic Fe(II) and nuclear staining (d, n). Prussian blue staining shows hemosiderin (i, j). Scale bars = 100 μm.

50 μM $FeCl_3$ up to 6 h, and decreased thereafter (Fig. 2B). We obtained similar results with the use of Fe(III)-NTA instead of $FeCl_3$.

3.4. Distinct responses of transferrin receptor 1 (TfR1) and ferroportin after iron loading in ESCs in vitro and in human specimens

After the treatment of ESCs with 0–100 μM Fe(III)-NTA for 6 h, TfR1 protein increased in a dose-dependent manner in all the ESCs (Fig. 3A). In a time-course study with 50 μM Fe(III)-NTA, TfR1 protein levels in n-euESCs and e-euESCs increased up to 12 h and decreased at 24 h. In contrast, TfR1 protein in ecESCs continuously increased up to 24 h (Fig. 3A). We obtained similar results with the use of $FeCl_3$ instead of Fe(III)-NTA.

In human specimens, TfR1 protein levels in the stromal cells of endometrium from ovarian endometriosis patients and endometriotic cysts were higher than in the stromal cells of normal endometrium (Fig. 3B). Ferroportin protein levels in the stromal cells of normal endometrium and endometrium of ovarian endometriosis were higher than in the stromal cells of endometriotic cysts, which showed almost no ferroportin (Fig. 3B). Ectopic endometrial stromal cells were confirmed with CD10 (Fig. 3B).

3.5. Transfer of catalytic ferrous iron from EpCs to ESCs

We then evaluated which cells, EpCs or ESCs, have a higher affinity for catalytic Fe(II). Either EpCs or ESCs were preloaded with

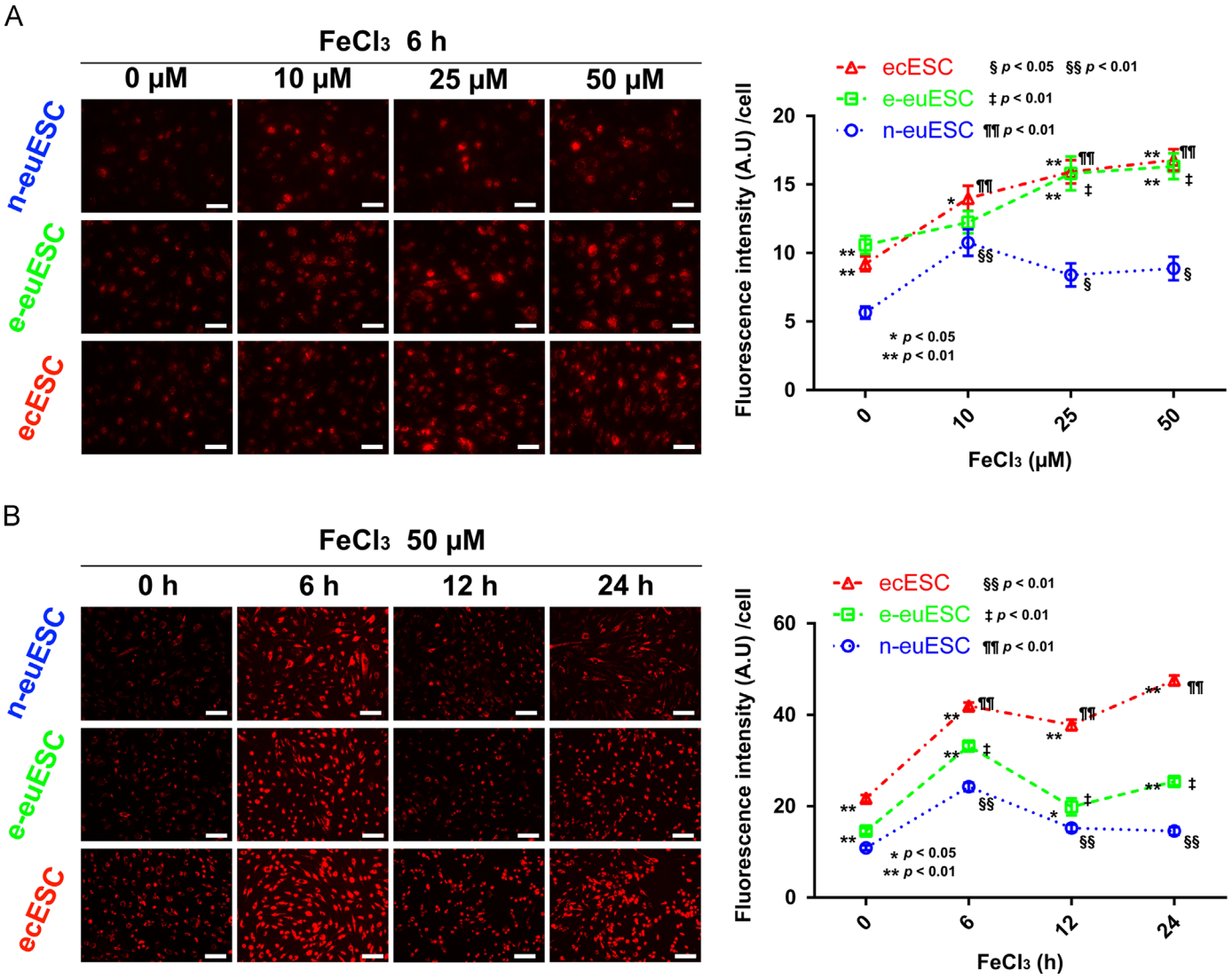

Fig. 2. Distinct catalytic Fe(II) response in endometriosis-associated stromal cells. We performed the detection of catalytic Fe(II) in immortalized ESCs. (A) HMRhoNox-M specific fluorescence in n-euESC, e-euESCs and ecESCs after treatment of 0, 10, 25 and 50 μM $FeCl_3$ for 6 h. We compared the fluorescence intensity (mean ± SEM) of each ESCs with the same dose of $FeCl_3$ and each dose in the same cell. Multiple comparisons with integrated fluorescence intensity per cell were performed using the Tukey HSD test to determine significant differences between each pair of cells. The statistics of a one-way ANOVA test were calculated using SPSS version 22.0 (SPSS Inc., Chicago, IL). Scale bars = 50 μm. * $p < 0.05$, ** $p < 0.01$ *vs* n-euESC; § $p < 0.05$, §§ $p < 0.01$, ‡ $p < 0.01$, ¶¶ $p < 0.01$ *vs* 0 μM. (B) HMRhoNox-M specific fluorescence in n-euESCs, e-euESCs and ecESCs after treatment with 50 μM $FeCl_3$ for 0, 6, 12 and 24 h. We compared the fluorescence intensity (mean ± SEM) of each ESCs with the same $FeCl_3$ treatment time and each treatment time in the same cell. Statistical analyses and the symbols are the same as in (A) except § $p < 0.05$, §§ $p < 0.01$, ‡ $p < 0.01$, ¶¶ $p < 0.01$ *vs* 0 h.

50 μM $FeCl_3$ and incubated for 12 h. ESCs were labeled with the green fluorescent cell tracker (CMFDA) and were co-cultured with EpCs thereafter. After an incubation of 6 h, we evaluated catalytic Fe (II) in EpCs and ESCs (Fig. 4A). Catalytic Fe(II) in ecESCs was significantly higher than that in EpCs, irrespective of iron loading (Fig. 4B). Under the cell culture conditions that ecESCs were incubated, where there was twice the number ecESCs as iron-loaded EpCs, catalytic Fe(II) in ecESCs was still significantly higher than in EpCs. However, under the conditions where the ratio of iron-loaded EpCs:ecESCs was 2:1, the amounts of catalytic Fe(II) in EpCs and ecESCs were not significantly different (Fig. 4C). Of note, in the co-culture experiment where ecESCs were replaced by either n-euESCs or e-euESCs, catalytic Fe(II) was retained in the EpCs or the amounts were not significantly different, respectively (Fig. 4D). Finally, we confirmed with siRNA experiments that the increased catalytic Fe (II) in ecESCs co-cultured with EpCs was dependent on TfR1. Silencing of TfR1 expression was confirmed with western blot analysis. After the knockdown of TfR1, the amounts of catalytic Fe(II) in EpCs and ecESCs were not significantly different (Fig. 4E).

4. Discussion

Although catalytic ferrous iron is important as an initiator of the Fenton reaction and has been implicated in various human pathologic conditions [34], methods to localize it were not available until recently [21,22]. Here, for the first time, we applied this method to human ovarian endometriosis, with special reference to the associated stromal cells [29]. For this method, frozen sections were required, based on our preliminary experiments.

Iron overload in ovarian endometriosis is thought to be a major pathogenic factor for carcinogenesis [4,6,35]. Thus, it is important to evaluate the presence of catalytic Fe(II) in these lesions. We observed abundant catalytic Fe(II), especially in the surrounding stromal cells facing endometriotic lumina (Fig. 1) where its amount was much higher than in the ESCs of control patients and the highest among the human specimens in the present study. Stromal cells in adenomyosis also showed higher catalytic Fe(II). Importantly, the distribution of catalytic Fe(II) was distinct from that of hemosiderin, which was generally present in macrophages

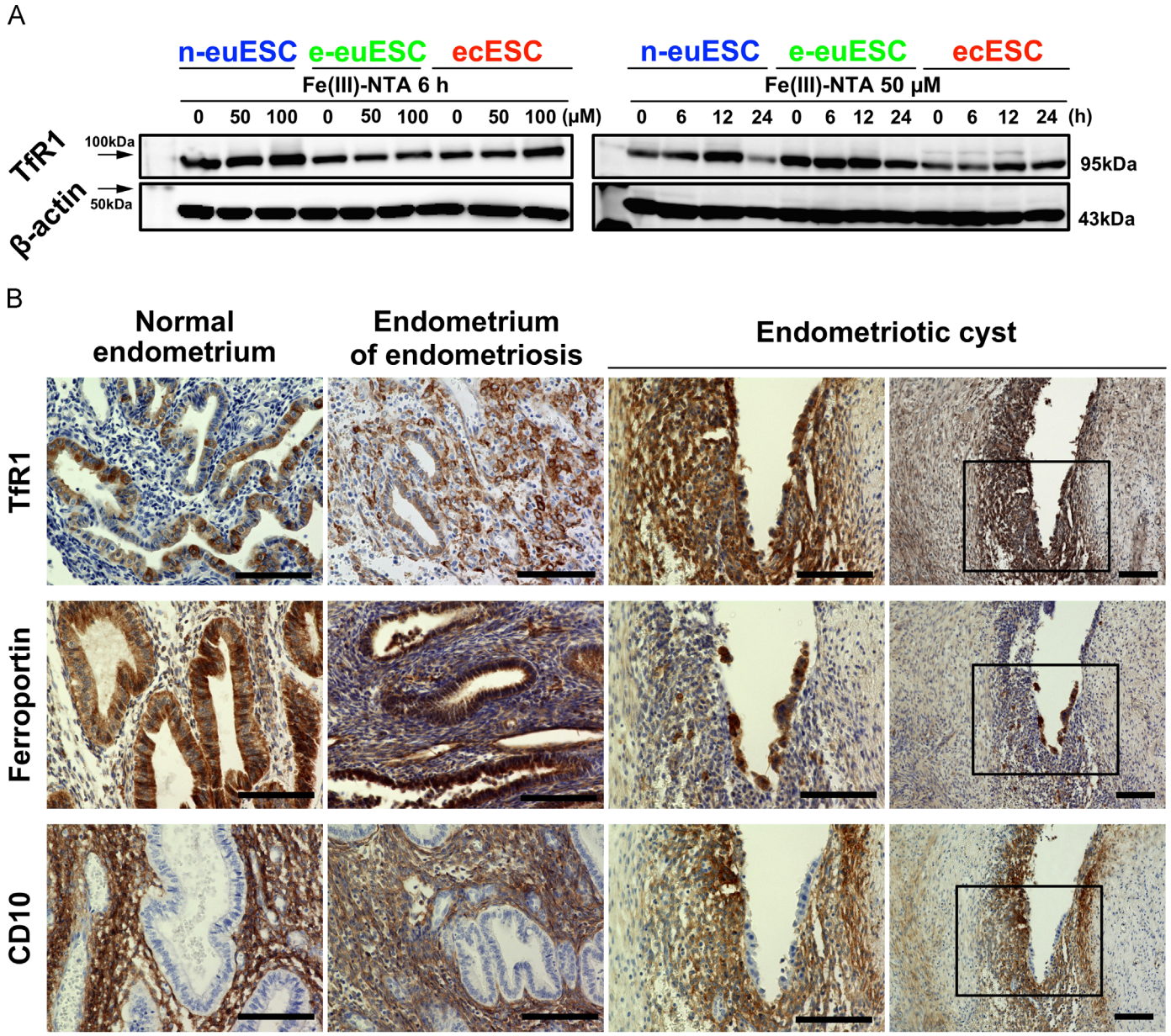

Fig. 3. Distinct responses of transferrin receptor 1 (TfR1) and ferroportin after iron loading in ESCs *in vitro* and in human specimens. (A) Protein levels of TfR1 in n-euESC, e-euESCs and ecESCs treated with 0, 50, 100 μM Fe(III)-NTA for 6 h were analyzed with western blot (left panels). Protein levels of TfR1 in n-euESCs, e-euESCs and ecESCs treated with 50 μM Fe(III)-NTA for 0, 6, 12, and 24 h were analyzed with western blot (right panels). Refer to the text for details. (B) Immunohistochemical analysis of TfR1 and ferroportin in normal endometrium, endometrium of endometriosis and endometriotic cysts. Refer to the text for details; scale bars = 100 μm.

as shown in our previous study [31].

We observed that catalytic Fe(II) of ESCs as seen by HMRho-Nox-M was located primarily in lysosomes and partially in mitochondria (Supplemental Fig. 1). In mammalian cells, serum transferrin that is filled with two Fe(III) atoms (holo-transferrin) binds to TfR1 on the plasma membrane and this complex is endocytosed and fuses with lysosomes [36]. Fe(III) that is incorporated as a transferrin/TfR1 complex is released and is immediately reduced to Fe(II) by STEAP3, followed by transport to the cytosol through DMT1, then to its final destination. The presence of Fe(II) is necessary for energy generation, heme synthesis in the mitochondria, DNA synthesis/repair and iron storage within the ferritin core [37–39]. Our data suggest that catalytic Fe(II) in ESCs is under physiological control but that lysosomal and mitochondrial iron pools would be larger during iron overload.

The present results using three different types of immortalized ESCs [29] showed intriguing results. Namely, ecESCs revealed significantly higher iron storing capacity as evidenced by higher amounts of catalytic Fe(II), not only under dose-dependent conditions but also time-dependent. e-euESCs showed some similarity to ecESCs (Fig. 2), which may partly explain the increased infertility in women of reproductive age with endometriosis. To explain this difference, we evaluated protein levels of TfR1 and ferroportin, the only iron exporter from cells. In ecESCs and e-euESCs, TfR1 levels continued to be higher in a time-course study whereas low TfR1 level presumably via feedback mechanism was evident for n-euESCs (Fig. 3A). We obtained similar results in human specimens for TfR1, where continued iron deposition is occurring via repeated monthly hemorrhage. Further, there was almost no ferroportin protein in the stromal cells surrounding endometriotic cysts, strengthening this "catalytic Fe(II)-abundant" situation, which was not observed in normal endometrium (Fig. 3B).

Oxidative stress via excess iron leads to genetic and epigenetic changes, uncontrolled cell growth, and abnormal intracellular

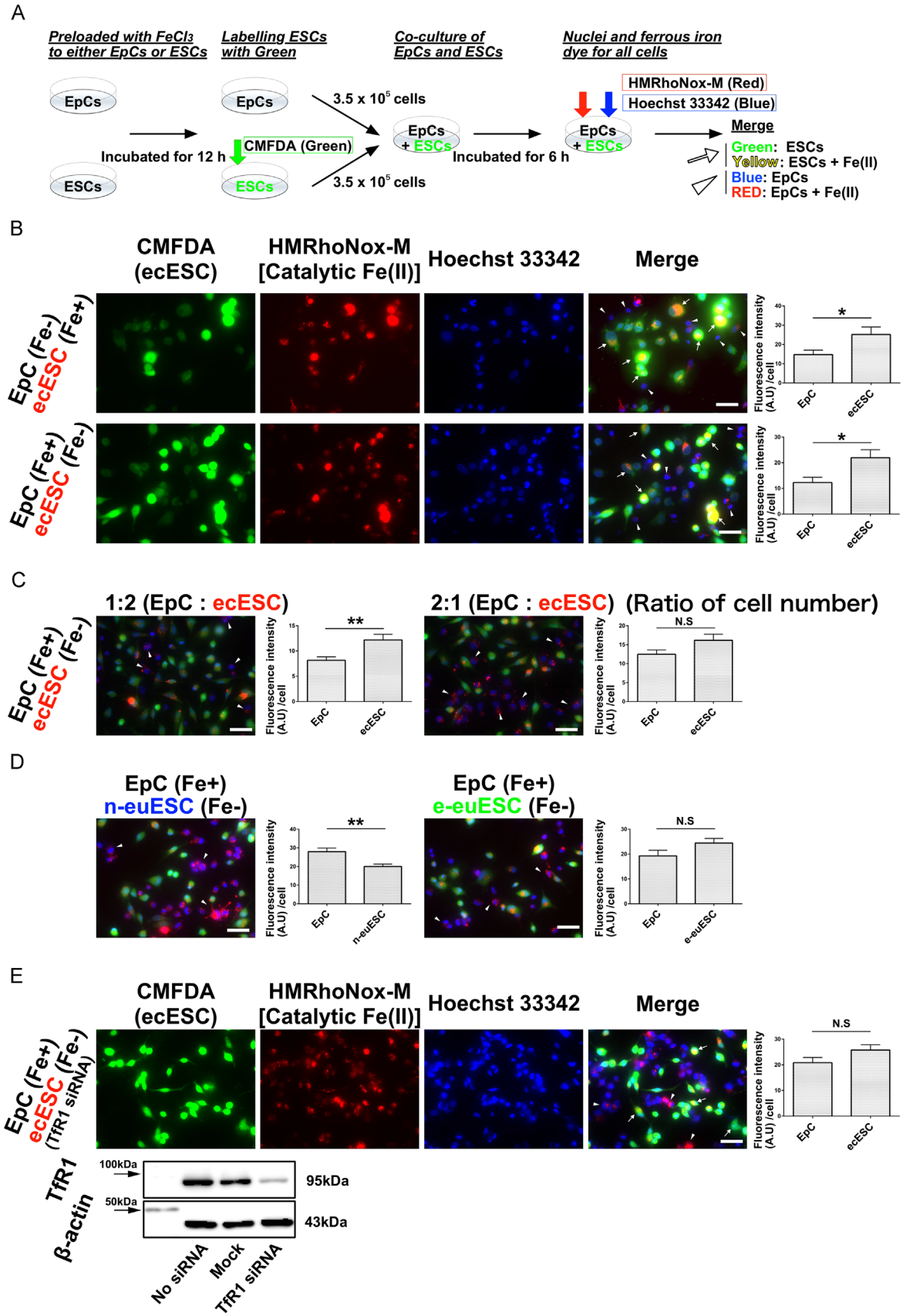

Fig. 4. ecESCs, not n-euESCs/e-euESCs, can receive catalytic Fe(II) from endometrial epithelial cells (EpCs) through TfR1. (A) The schema for the current co-culture method of EpCs and ESCs. (B) Co-culture of ecESCs preloaded with $FeCl_3$ and EpCs that were not preloaded with $FeCl_3$ (upper row, $p=0.029$). Co-culture of EpCs preloaded with $FeCl_3$ and ecESCs that were not preloaded with $FeCl_3$ (bottom row, $p=0.012$). Total seeded cell number was 7.0×10^5 cells (3.5×10^5 EpCs and 3.5×10^5 ecESCs). Arrows, ecESCs; arrowheads, EpCs. Fluorescence intensity of HMRhoNox-M in EpCs and ecESCs was expressed as the mean ± SEM; scale bars=50 μm. (C) Altering the ratio of EpCs and ecESCs (left: 4.0×10^5 EpCs and 8.0×10^5 ecESCs, $p=0.003$; right: 8.0×10^5 EpCs and 4.0×10^5 ecESCs, $p=0.065$). Arrowheads, EpCs; scale bars=50 μm; NS, not significant. (D) Co-culture of EpCs and n-euESCs ($p=0.001$), and EpCs and e-euESCs ($p=0.083$). Total seeded cell number was 7.0×10^5 cells (3.5×10^5 EpCs and 3.5×10^5 euESCs). Arrowheads, EpCs; scale bars=50 μm; NS, not significant. (E) Co-culture of EpCs preloaded with $FeCl_3$ and ecESCs, transfected with TfR1 siRNA but not preloaded with $FeCl_3$ ($p=0.095$). Western blotting analysis confirms the knockdown of TfR1 in ecESCs. Arrows, ecESCs; arrowheads, EpCs; scale bars=50 μm. (B-E) * $p<0.05$, ** $p<0.01$, NS, not significant; unpaired Student's *t*-test.

signaling [7,16,40,41]. Therefore, endometriosis might be a disorder of TfR1 dysregulation through ron regulatory protein 1 (IRP1) or iron regulatory protein 2 (IRP2) in the cytosol. Surprisingly, similar traits for iron manipulation are retained in the three different types of immortalized ESCs. We believe that the regulation of TfR1 message via the IRP1 or IRP2 in the case of iron excess works appropriately in n-euESCs and e-euESCs. However, this does not work in ecESCs. In a previous experiment, we reported overexpression of IRP1/IRP2 and FBXL5 in ecESCs [31]. Abundant IRP1/IRP2 appears to be associated with the signaling for "iron uptake." A more precise description of the mechanism requires further experiments.

Finally, we performed a study to determine which cell, EpCs or ESCs, has a higher affinity for iron. Notably, only ecESCs, not e-euESCs or n-euESCs, revealed a significantly more intense affinity for iron over EpCs, and ecESCs could receive excess iron from EpCs via TfR1 (Fig. 4). Thus far, we are not able to conclude whether direct cell contact is necessary or not. Mesenchymal cells, such as muscle and blood cells, originally derived from mesoderm, have a high affinity for iron. ESCs are derived from mesenchymal cells. We therefore speculate that ecESCs regained this original characteristic of mesodermal cells by genetic/epigenetic processes. It is generally accepted that ecESCs play a role in the progression of endometriosis via cytokine production [42]. However, the present study demonstrates that ecESCs play a role, at least in part, in preventing endometrial epithelial cells from excess iron-mediated oxidative DNA damage leading to carcinogenesis.

There are two limitations in the present study. Catalytic Fe(II) is completely dependent on HMRhoNox-M probe, which is accumulated mainly in lysosomes. Thus, we cannot rule out the possibility that distribution and amounts of catalytic Fe(II) may be different in other organelles including nucleus. We used Ishikawa endometrioid carcinoma cells as a model of endometrial epithelial cells.

There are two clinical indications, as well. An abundance of stromal cells with a deficiency in epithelial cells in ovarian endometriosis reveals a theoretical low risk for carcinogenesis, and *vice versa*. If we can generate ecESCs from other somatic cells, presumably via *i*PS cell technique, transplantation of those cells may work to collect excess iron from epithelial/mesothelial cells to prevent carcinogenesis [43].

5. Conclusion

We showed, for the first time, that catalytic ferrous iron is abundant in endometriotic lesions, which is, at least in part, dependent on alterations in the expression of TfR1 and ferroportin. Furthermore, we demonstrated that ectopic stromal cells revealed distinct iron metabolism for storage of excess iron and could receive excess iron from epithelial cells.

Competing interests

The authors have no conflicts of interest to disclose.

Acknowledgments

This work was supported, in part, by the National Cancer Center Research and Development Fund (25-A-5) and a Grant-in-aid for research from the Ministry of Education, Culture, Sports, Science and Technology (MEXT) of Japan (24390094; 221S0001-04; 24108001).

Appendix A. Supplementary Information

Supplementary data associated with this article can be found in the online version at http://dx.doi.org/10.1016/j.redox.2015.10.001.

References

[1] R.O. Burney, L.C. Giudice, Pathogenesis and pathophysiology of endometriosis, Fertil Steril 98 (2012) 511–519.
[2] L.C. Giudice, L.C. Kao, Endometriosis, Lancet 364 (2004) 1789–1799.
[3] S.E. Bulun, Endometriosis, N. Engl. J. Med. 360 (2009) 268–279.
[4] H. Kobayashi, K. Sumimoto, N. Moniwa, M. Imai, K. Takakura, T. Kuromaki, et al., Risk of developing ovarian cancer among women with ovarian endometrioma: a cohort study in Shizuoka Japan, Int. J. Gynecol. Cancer 17 (2007) 37–43.
[5] C.L. Pearce, C. Templeman, M.A. Rossing, A. Lee, A.M. Near, P.M. Webb, et al., Association between endometriosis and risk of histological subtypes of ovarian cancer: a pooled analysis of case-control studies, Lancet Oncol. 13 (2012) 385–394.
[6] S. Toyokuni, Role of iron in carcinogenesis: cancer as a ferrotoxic disease, Cancer Sci. 100 (2009) 9–16.
[7] S. Toyokuni, Iron and thiols as two major players in carcinogenesis: friends or foes? Front Pharmacol. (2014) 5.
[8] J.M. Wriggleworth, H. Baum, The biochemical function of iron, in: A. Jacobs, M. Worwood (Eds.), Iron in Biochemistry and Medicine, Academic Press, London, 1980, pp. 29–86 , II.
[9] R. Jiang, J.E. Manson, J.B. Meigs, J. Ma, N. Rifai, F.B. Hu, Body iron stores in relation to risk of type 2 diabetes in apparently healthy women, J. Am. Med. Asoc. 291 (2004) 711–717.
[10] D. Schuppan, N.H. Afdhal, Liver cirrhosis, Lancet 371 (2008) 838–851.
[11] Fenton HJH, Oxidation of tartaric acid in presence of iron, J. Chem. Soc. 65 (1894) 899–910.
[12] S.S. Leonard, G.K. Harris, X. Shi, Metal-induced oxidative stress and signal transduction, Free Radic. Biol. Med. 37 (2004) 1921–1942.
[13] S. Toyokuni, J.-L. Sagripanti, DNA single- and double-strand breaks produced by ferric nitrilotriacetate in relation to renal tubular carcinogenesis, Carcinogenesis 14 (1993) 223–227.
[14] S. Toyokuni, T. Mori, M. Dizdaroglu, DNA base modifications in renal chromatin of Wistar rats treated with a renal carcinogen, ferric nitrilotriacetate, Int. J. Cancer 57 (1994) 123–128.
[15] S. Toyokuni, Reactive oxygen species-induced molecular damage and its application in pathology, Pathol. Int. 49 (1999) 91–102.
[16] J.C. Lee, Y.O. Son, P. Pratheeshkumar, X. Shi, Oxidative stress and metal carcinogenesis, Free Radic. Biol. Med. 53 (2012) 742–757.
[17] K. Yamaguchi, M. Mandai, S. Toyokuni, J. Hamanishi, T. Higuchi, K. Takakura, et al., Contents of endometriotic cysts, especially the high concentration of free iron, are a possible cause of carcinogenesis in the cysts through the iron-induced persistent oxidative stress, Clin. Cancer Res. 14 (2008) 32–40.
[18] M. Mandai, N. Matsumura, T. Baba, K. Yamaguchi, J. Hamanishi, I. Konishi, Ovarian clear cell carcinoma as a stress-responsive cancer: influence of the microenvironment on the carcinogenesis and cancer phenotype, Cancer Lett. 310 (2011) 129–133.
[19] S. Toyokuni, Iron-induced carcinogenesis: the role of redox regulation, Free Radic. Biol. Med. 20 (1996) 553–566.
[20] M. Gerlinger, A.J. Rowan, S. Horswell, J. Larkin, D. Endesfelder, E. Gronroos, et al., Intratumor heterogeneity and branched evolution revealed by multiregion sequencing, New Engl. J. Med. 366 (2012) 883–892.
[21] T. Hirayama, K. Okuda, H. Nagasawa, A highly selective turn-on fluorescent probe for iron (II) to visualize labile iron in living cells, Chem. Sci. 4 (2013) 1250–1256.
[22] T. Mukaide, Y. Hattori, N. Misawa, S. Funahashi, L. Jiang, T. Hirayama, et al., Histological detection of catalytic ferrous iron with the selective turn-on fluorescent probe RhoNox-1 in a Fenton reaction-based rat renal carcinogenesis model, Free Radic. Res. 48 (2014) 990–995.
[23] Y. Hattori, T. Mukaide, L. Jiang, T. Kotani, H. Tsuda, Y. Mano, et al., Catalytic ferrous iron in amniotic fluid as a predictive marker of human maternal-fetal disorders, J. Clin. Biochem. Nutr. 56 (2015) 57–63.
[24] M. Niwa, T. Hirayama, K. Okuda, H. Nagasawa, A new class of high-contrast Fe (II) selective fluorescent probes based on spirocyclized scaffolds for visualization of intracellular labile iron delivered by transferrin, Org. Biomol. Chem. 12 (2014) 6590–6597.
[25] G.D. Orvis, R.R. Behringer, Cellular mechanisms of Mullerian duct formation in the mouse, Dev. Biol. 306 (2007) 493–504.
[26] C.A. Stewart, Y. Wang, M. Bonilla-Claudio, J.F. Martin, G. Gonzalez, M. M. Taketo, et al., CTNNB1 in mesenchyme regulates epithelial cell differentiation during Mullerian duct and postnatal uterine development, Mol. Endocrinol. 27 (2013) 1442–1454.
[27] A. Banas, T. Teratani, Y. Yamamoto, M. Tokuhara, F. Takeshita, G. Quinn, et al., Adipose tissue-derived mesenchymal stem cells as a source of human hepatocytes, Hepatology 46 (2007) 219–228.
[28] S. Toyokuni, K. Uchida, K. Okamoto, Y. Hattori-Nakakuki, H. Hiai, E. R. Stadtman, Formation of 4-hydroxy-2-nonenal-modified proteins in the

renal proximal tubules of rats treated with a renal carcinogen, ferric nitrilotriacetate, Proc. Natl. Acad. Sci. U. S. A. 91 (1994) 2616–2620.
[29] A. Iwase, H. Ando, T. Nagasaka, D. Shibata, T. Harata, Y. Shimomura, et al., Neutral endopeptidase expressed by decidualized stromal cells suppresses akt phosphorylation and deoxyribonucleic acid synthesis induced by endothelin-1 in human endometrium, Endocrinology 147 (2006) 5153–5159.
[30] Y. Yamashita, T. Tsurumi, N. Mori, T. Kiyono, Immortalization of Epstein-Barr virus-negative human B lymphocytes with minimal chromosomal instability, Pathol. Int. 56 (2006) 659–667.
[31] H. Kobayashi, Y. Yamashita, A. Iwase, Y. Yoshikawa, H. Yasui, Y. Kawai, et al., The ferroimmunomodulatory role of ectopic endometriotic stromal cells in ovarian endometriosis, Fertil. Steril. 98 (415-22) (2012), e1-12.
[32] Y. Suzuki, K. Shibata, F. Kikkawa, H. Kajiyama, K. Ino, S. Nomura, et al., Possible role of placental leucine aminopeptidase in the antiproliferative effect of oxytocin in human endometrial adenocarcinoma, Clin. Cancer Res. 9 (2003) 1528–1534.
[33] T. Nakahara, A. Iwase, T. Nakamura, M. Kondo, Bayasula, Kobayashi H et al. Sphingosine-1-phosphate inhibits H_2O_2-induced granulosa cell apoptosis via the PI3K/Akt signaling pathway, Fertil. Steril. 98 (1001-8) (2012) e1.
[34] B. Halliwell, J.M.C. Gutteridge, Free radicals in biology and medicine, 4 ed., Oxford University Press, New York, 2007.
[35] Y. Yamashita, S. Akatsuka, K. Shinjo, Y. Yatabe, H. Kobayashi, H. Seko, et al., Met is the most frequently amplified gene in endometriosis-associated ovarian clear cell adenocarcinoma and correlates with worsened prognosis, PLoS One 8 (2013) e57724.
[36] J. Huotari, A. Helenius, Endosome maturation, EMBO J. 30 (2011) 3481–3500.
[37] D.R. Richardson, P. Ponka, The molecular mechanisms of the metabolism and transport of iron in normal and neoplastic cells, Biochim. Biophys. Acta 1331 (1997) 1–40.
[38] D.R. Richardson, D.J. Lane, E.M. Becker, M.L. Huang, M. Whitnall, Y. Suryo Rahmanto, et al., Mitochondrial iron trafficking and the integration of iron metabolism between the mitochondrion and cytosol, Proc. Natl. Acad. Sci. U. S. A. 107 (2010) 10775–10782.
[39] S.V. Torti, F.M. Torti, Iron and cancer: more ore to be mined, Nat. Rev. Cancer 13 (2013) 342–355.
[40] T. Tanaka, S. Kondo, Y. Iwasa, H. Hiai, S. Toyokuni, Expression of stress-response and cell proliferation genes in renal cell carcinoma induced by oxidative stress, Am. J. Pathol. 156 (2000) 2149–2157.
[41] S. Akatsuka, Y. Yamashita, H. Ohara, Y.T. Liu, M. Izumiya, K. Abe, et al., Fenton reaction induced cancer in wild type rats recapitulates genomic alterations observed in human cancer, PLoS One 7 (2012) e43403.
[42] J.F. Tseng, I.P. Ryan, T.D. Milam, J.T. Murai, E.D. Schriock, D.V. Landers, et al., Interleukin-6 secretion in vitro is up-regulated in ectopic and eutopic endometrial stromal cells from women with endometriosis, J. Clin. Endocrinol. Metab. 81 (1996) 1118–1122.
[43] S. Toyokuni, Iron as a target of chemoprevention for longevity in humans, Free Radic. Res. 45 (2011) 906–917.